Thiol-stabilized Gold Nanoparticles: new ways to displace thiol-layers using Yttrium or Lanthanide Chlorides

Julie P. Vanegas, Juan C. Scaiano and Anabel E. Lanterna**

Department of Chemistry and Biomolecular Sciences and Centre for Catalysis Research and Innovation. University of Ottawa. 10 Marie Curie, Ottawa, ON. K1N 5N6. Canada.

KEYWORDS. Gold, nanoparticles, thiol ligands, lanthanides, yttrium.

ABSTRACT. We use the aurophilic interactions shown by lanthanides to overcome the sulfur-gold interaction. UV-Vis and XPS spectroscopy confirm that Yttrium or lanthanide chlorides easily displace sulfur ligands from the surface of thiol-stabilized gold nanoparticles.

INTRODUCTION

The modification of gold surfaces with thiol derivatives has been extensively explored[1, 2, 3, 4] in the past two decades since the first report in 1993 by Mulvaney and Giersig[5] and the very well-known Brust-Schiffrin bi-phasic method developed in 1994.[6] The thiolate bond resulting from sulfur-gold interaction has proven even stronger than the gold-gold metallic bond[7] and therefore the modification of gold surfaces, particularly gold nanoparticles (AuNPs), with thiolate ligands is considered the most stable passivation method for AuNPs.[8, 9, 10] The exchange of ligands at the

AuNPs surface has been studied as many applications need to recover either the ligand,[11] the AuNP or both.[12, 13] Aurophilic interactions between the surface of gold nanoclusters (AuNCs) and lanthanides, namely Ln^{3+}-Au^{+}, have recently been reported.[14] However, the relative strength of the Ln^{3+}-Au^{+} interaction is still unknown, especially compared to the well-known stability of the sulfur-gold bond. Here, we use lanthanides as a new chemical strategy for sulfur ligand displacement from thiol-stabilized AuNPs.

Nowadays, the use of lanthanides is mainly related to the formation of up-conversion nanoparticles for bioanalytical applications.[15, 16] The inner electronic configuration of these elements is suitable for electronic excitation that gives rise to the photon-upconversion process. It is known that some lanthanides can form complexes with carbonyl groups, and to the best of our knowledge no interactions with sulphur moieties have been reported.[17, 18, 19, 20]

Herein we present our efforts to demonstrate that thiol-capped AuNPs can undergo ligand release in the presence of a RE salt. UV-vis and XPS analysis prove that the sulfur material is released from the surface of the Au nanostructure upon addition of RE salts, possibly through the mechanism proposed in Scheme 1.

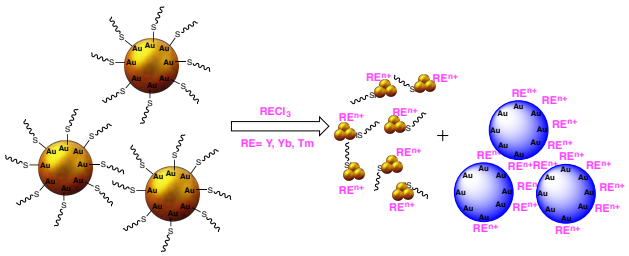

Scheme 1. Thiol-capped Au nanostructures undergo ligand release in the presence of rare earth ions (RE^{n+}) inducing particle agglomeration and possible concomitant Au-Au bond rupture.

EXPERIMENTAL SECTION

Synthesis of AuNPs@thiol. Thiol-capped AuNPs were prepared by thiol ligand exchange of the precursor AuNPs capped with citrate. Thus, citrate-capped AuNPs (AuNPs@C) were synthesized from $HAuCl_4$ according to a reported procedure[21] using sodium citrate as both reducing and capping agent. Briefly, 40 mg (0.10 mmol) of $HAuCl_4 \bullet 3H_2O$ were mixed together with 200 mg (0.68 mmol) of $Na_3C_6H_5O_7$ and dissolved in 500 mL of milliQ water. The solution was boiled for 1 h. The resulting colloidal solution exhibits the typical plasmon band at λ_{max} around 525 nm and an average core diameter of (12 ± 2) nm. Then, 0.063 mmol of the thiol were added to 15 mL of the AuNPs@C and stirring for 24 h. Particles were purified by two subsequent processes of centrifugation at 11,000 rpm followed by milliQ water rinse and finally re-dispersed in water. The resulting colloidal solutions were characterized by UV-vis spectroscopy and TEM. The amount of thiol in the final solution was determined by subtraction of the amount of thiol recovered from the initial concentration.

Thiol displacement. The release of the sulfur moieties was performed by adding an aliquot of the rare earth (RE) salt ($YCl_3 \bullet 6H_2O$ 4 mM, $YbCl_3 \bullet 6H_2O$ 2.6 mM or $TmCl_3 \bullet 6H_2O$ 2.6 mM) to the corresponding Au nanostructure. Briefly, subsequent additions of 10 μL of the YCl_3 (or $YbCl_3$ or $TmCl_3$) solution were added to 2 mL of AuNPs@thiols and the UV-vis spectra were collected after each addition.

Ionic strength effect. In order to rule out the effect of the ionic strength change, the AuNPs@thiols (or AuNPs@citrate) were mixed with NaCl solutions of different concentrations reaching the same or higher ionic strength than in the case of RE salts. The ionic strength was calculated as $I = \frac{1}{2}\sum_{i=1}^{n} c_i z_i^2$

RESULTS AND DISCUSSION

As is well known, thiol compounds have strong affinity for Au surfaces due to the formation of a strong Au–S bond; [7, 21] however, we show here that the Au surface thiol passivation can be defeated in the presence of RE ions. In order to test this hypothesis, three thiols carrying different moieties were used to passivate Au nanostructures: 2-mercaptoethanol (S-ETH), 7-mercapto-4-methylcoumarin (S-COU) and 11-mercaptoundecanoic acid (S-MUA) (Scheme 2). The diverse chemical properties of the thiols selected would help to show the extent of this methodology. Subsequently, AuNPs were subjected to ligand displacement in the presence of RE salts Yttrium (YCl_3), Ytterbium ($YbCl_3$) and Thulium ($TmCl_3$) and studied by UV-vis and XPS spectroscopy.

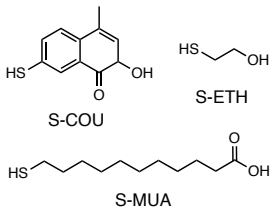

Scheme 2. Thiols used in this work.

Thiol-capped gold nanomaterials were prepared in our lab as described in the experimental section. Briefly, thiol-aged gold NPs were produced by overnight incubation of citrate-stabilized AuNPs with the corresponding thiol in order to ensure complete ligand exchange (i.e. citrate replaced by thiol) maintaining the stability of the colloid. Residual RSH were removed by several centrifugation and washing cycles. Figure S1 shows the UV–vis spectra of the three AuNPs@thiolate studied here. Plasmon resonance band at maximum around 528 nm and 530 nm are identified for AuNPs@S-COU and AuNPs@S-MUA, respectively. AuNPs@S-ETH presents two plasmon resonance bands around 530 nm and 693 nm, most likely because of the change of interspacing distance between AuNPs due to the small dimensions of this ligand.[22] TEM imaging (Figure S2) shows that the thiol-capped AuNPs prepared after thiol ligand exchange of the

AuNPs@C remain as nearly monodisperse spheres with an average size of about (14 ± 3) nm. In particular, AuNPs@S-ETH show more agglomeration in accordance with their UV-vis spectra (See ESI).

After addition of RE salts, the plasmon resonance bands of the three different thiol-capped AuNPs are red shifted, as seen in Figure 1, which compares the UV-Vis absorption spectra of AuNPs@S-ETH, AuNPs@S-COU and AuNPs@S-MUA nanoparticles in water when different concentrations of Yttrium chloride were added. Similar results were found when other lanthanide salts were used (See Figure S3 – S5 for Thulium and Ytterbium salts). Figure 1 also shows the corresponding change in the absorption versus the concentration of the RE salt. A sigmoidal fitting of those results shows how easily the AuNP can change its plasmon band in the presence of the lanthanide salts; thus the inflexion point of those curves can be correlated to a critical concentration of Yttrium (or other lanthanides) necessary to detect a significant change on the UV-Vis spectra. Table 1 summarizes the critical concentrations found for each particle/lanthanide combination. It is important to notice that the amount of lanthanide needed is in all cases at least ten times lower than the amount of thiol per NP (notice for example the average S-ETH/RE is 66), suggesting lanthanides have a great ability to interact with the passivated-Au surface. In particular, AuNPs@S-ETH and AuNPs@S-COU are more sensitive to the amount of lanthanide salt added. Among all the thiol-capped AuNPs, AuNPs@S-MUA are less prone to modification of the plasmon band (Figure 1B-D), probably due to lower surface accessibility associated with the length of the ligand chain[23] which hinders the particle surface from interacting with incoming ligands. Also, the ligand carbonyl groups near the surface could complex with lanthanides

as previously demonstrated.[17, 18] These phenomena can also be followed by the changes on the solution color, gradually shifting from red to blue (Figure 1 insets). Additionally, the AuNPs@C, used as the precursor for the other thiolated-AuNPs, were also mixed with lanthanides salts as a control experiment. Interestingly, citrate coated nanoparticles are very stable upon addition of RE salts, concentrations around 10 times higher than those needed in order to cause similar changes in the UV-Vis spectra (Figure 2, Figure S6 and Table 1). Interaction between citrate and RE salts are known[24] and might be interfering with the interaction of RE ions with the gold surface. This suggests that ligand exchange depends strongly on the interaction of the RE salts and thiol groups at the Au surface. Finally, electrostatic effects[25] were ruled out by comparing addition of NaCl at the same ionic strength used with YCl_3, which does not affect the plasmon absorption band (Figure S7-S8).

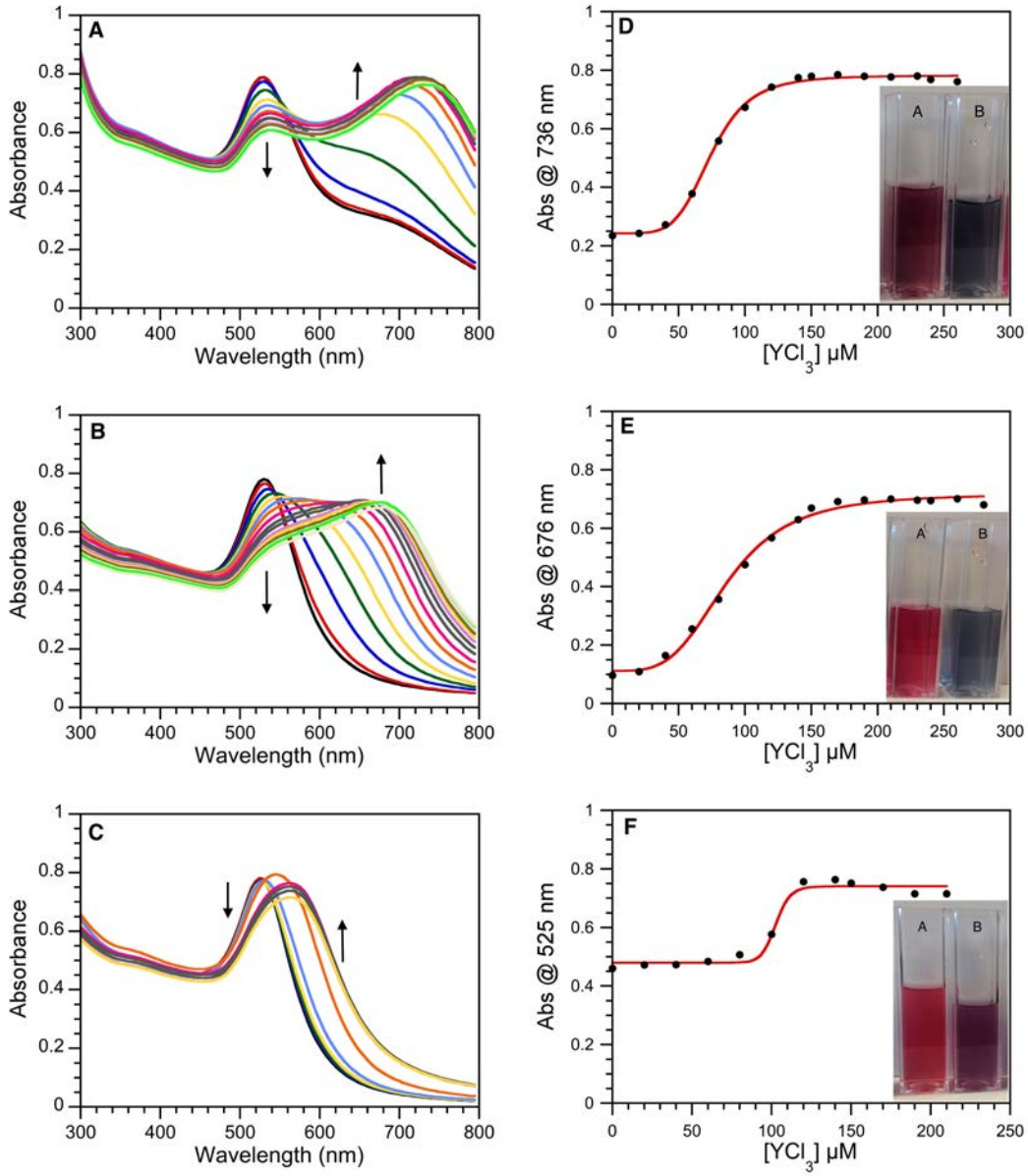

Figure 1. UV-Vis absorption spectra (*left*) and plots of the absorption versus YCl_3 concentration (*right*) for A-D) AuNPs@S-ETH, B-E) AuNPs@S-COU, and C-F) AuNPs@S-MUA. Insets: A) Thiol-capped AuNPs, B) AuNPs in the presence of YCl_3.

Table 1. Critical concentration of the lanthanide (or Yttrium) salt for each particle and the concentration ratios between thiol, lanthanide, and AuNps.

Ligand	**S-ETH**	**S-COU**	**S-MUA**	**Citrate**
Thiol/NP (x10^4)	140	84	46	-
[YCl_3] (μM)	75	87	99	1482
YCl_3/NP (x10^4)	2.7	3.1	5.6	53.6
Thiol/Y	54	28	14	-
[$YbCl_3$] (μM)	59	74	76	780
$YbCl_3$/NP (x10^4)	2.1	2.7	2.8	28.2
Thiol/Yb	69	33	18	-
[$TmCl_3$] (μM)	54	71	67	715
$TmCl_3$/NP (x10^4)	2.0	2.6	2.4	25.9
Thiol/Tm	76	35	20	

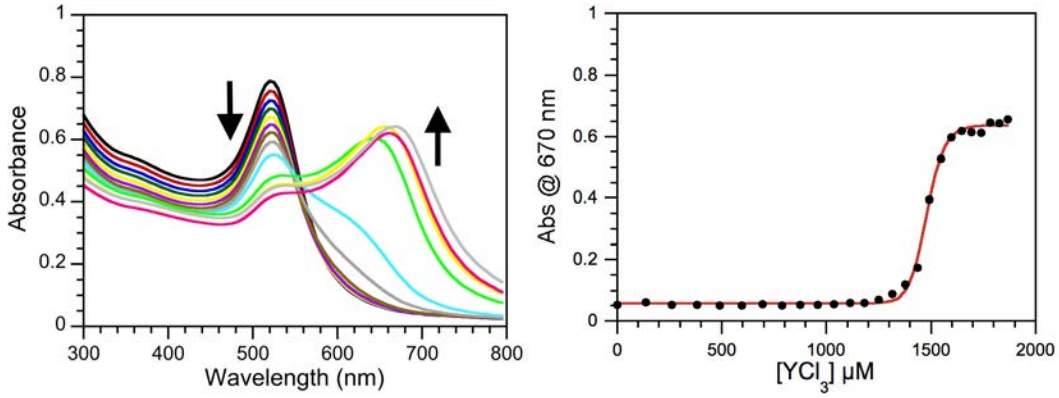

Figure 2. UV-Vis absorption spectra (*left*) and plot of the absorption versus YCl_3 concentration for AuNPs@C.

In order to confirm that the drastic change on the plasmon resonance band of the thiol-capped AuNPs is due to the displacement of thiol-ligands, we analysed the resulting NPs by High-

Resolution X-ray Photon Spectroscopy (HR-XPS). First we analyse the Au 4f region, in order to determine the oxidation state of the Au species. Figure 3 shows that Au 4f signals shift towards binding energies (BE) that are higher (more oxidized Au species) when AuNPs surface is surrounded by Y or S-ETH (See tables 2 and S1) rather than citrate. Thus, increasing BE are expected for capping agents ranging from citrate to thiols to RE ions. When the particles are treated with YCl_3 (similar results where found with $YbCl_3$ and $TmCl_3$), they are subjected to centrifugation and several washes before XPS analysis. Figure 4 shows the Au 4f HR XPS spectra obtained before and after addition of the RE salts, for the resulting pellet (AuNPs precipitate) and supernatant. As expected for Au-RE interactions, the Au signals corresponding to the AuNPs precipitate shift toward higher BE. When AuNPs@thiols are treated with $YbCl_3$, Au species can be also detected in the supernatant. Interestingly enough, these species show higher oxidation than the Au species found in the pellet, suggesting that these Au species are different from those found in the AuNPs. This could support the mechanism described in Scheme 1 where Au atoms are also displaced from the AuNPs surface. When YCl_3 or $TmCl_3$ are used, gold species are not found in the supernatant, although the presence of trace amounts cannot be ruled out. The characteristic S 2p signals (S 2p3/2 about 162.05 eV) displayed for each thiol-stabilized AuNPs are in agreement with gold-thiolate bonding (Figure S9).[26, 27, 28, 29] In the case of AuNPs@S-ETH and AuNPs@MUA, BE signals above 164 eV account for the presence of more oxidized sulfur compounds (not seen in the case of AuNPs@COU; Figure S9B). When treated with lanthanide ions, the thiol-stabilized AuNPs release more reduced sulfur species. Figure 5 shows the HR XPS spectra in the S 2p region found for AuNPs@S-ETH upon treatment with Y, Yb or Tm chlorides. Although sulfur species can still be found in the AuNPs precipitate, there is no doubt about the presence of a large amount of released sulfur species in the

supernatant. Interestingly enough, the S 2p signals found in the latter correspond to more reduced sulfur species as can be inferred from the more intense peak found around 164 eV. Evidence for the presence of Yttrium in both the pellet and the supernatant is obtained by looking at the characteristic Y 3d BE signals between 150-162 eV (notice that their coincides with the S 2p region, Figure 5A). [30, 31] The same was also found for Yb and Tm (Table S1). Table 2 summarizes the XPS results obtained for each particle after addition of YCl_3 (See Table S1 for $YbCl_3$ and $TmCl_3$). It is important to note that the presence of sulfur compounds in the supernatant was confirmed in the cases of S-ETH and S-COU, but cannot be ruled out when S-MUA was used, more likely due to a lower amount of displaced ligand. This is in agreement with the lower interaction seen by UV-vis spectroscopy when AuNPs@SMUA are used.

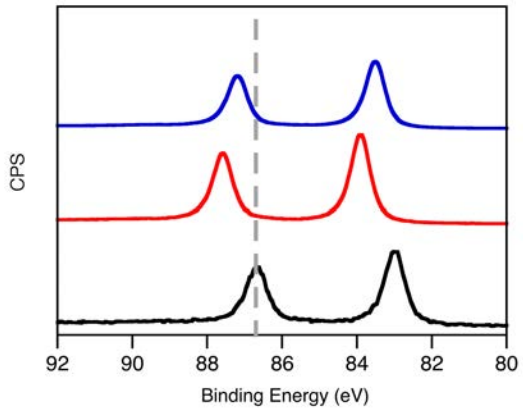

Figure 3. Au 4f HR XPS spectra for AuNPs surrounded by citrate (black), YCl_3 (red) and S-ETH (blue).

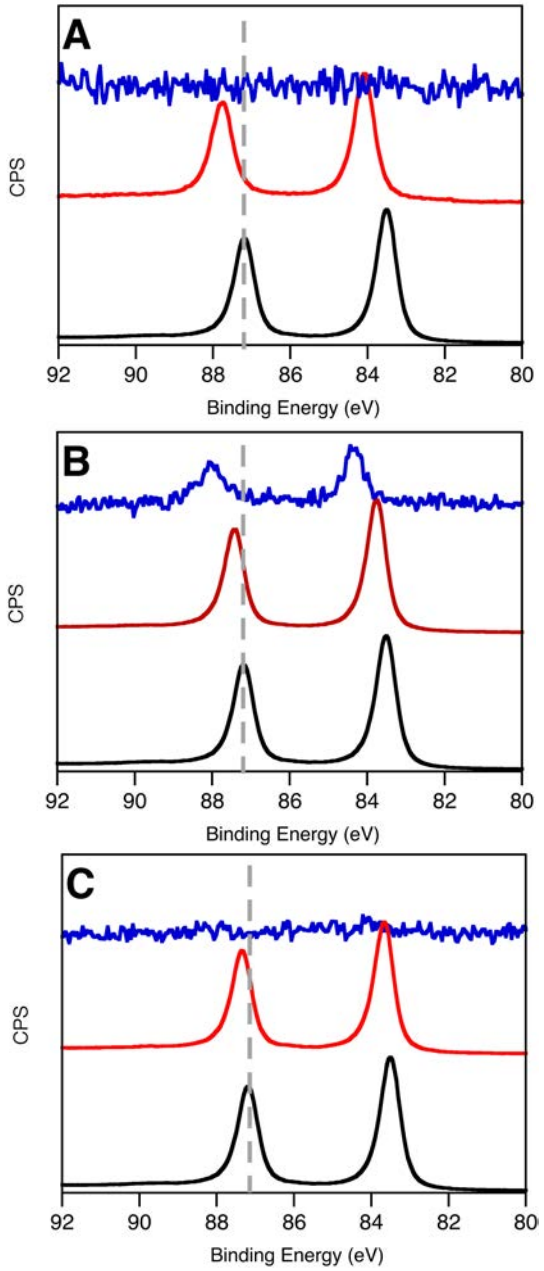

Figure 4. Au 4f HR XPS spectra for AuNPs@S-ETH before (black) and after addition of $RECl_3$ pellet (red) and supernatant (blue). A) YCl_3 (~250 μM) B) $YbCl_3$ (~130 μM) and C) $TmCl_3$ (~160 μM).

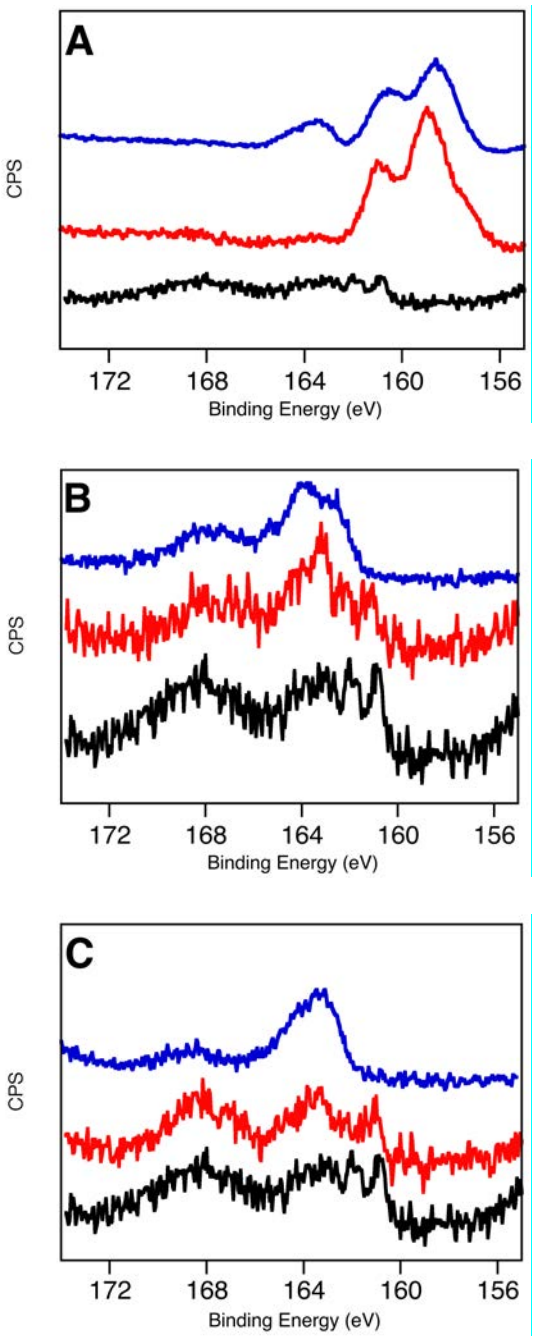

Figure 5. S 2p HR XPS spectra for AuNPs@S-ETH before (black) and after addition of ~200 μM $RECl_3$ pellet (red) and supernatant (blue). A) YCl_3, B) $YbCl_3$ and C) $TmCl_3$.

Table 2. XPS data of AuNPs@thiol/YCl_3 systems.

Sample	Binding Energy (eV)		
	Au $4f_{5/2}$	Y $3d_{3/2}$	S $2p_{1/2}$
AuNPs@S-ETH	87.2	-	168.3 / 162.7
AuNPs@S-ETH+YCl_3 P	87.8	160.8 /157.3	ND
AuNPs@S-ETH+YCl_3 SN	ND	160.9 / 154	164.9
AuNPs@S-COU	87.5	-	163.3
AuNPs@S-COU+YCl_3 P	88.0	160.5 / 153.7	163.7
AuNPs@S-COU+YCl_3 SN	ND	160.9 / 154.0	164.9
AuNPs@S-MUA	87.1	-	164.7 / 169.7
AuNPs@S-MUA + YCl_3 P	87.7	160.2 / 154.6	167.4 / 163.7
AuNPs@S-MUA + YCl_3 SN	ND	160.2 / 152	162.9

Binding energy (eV) for the principal elements in eV; referenced to aliphatic carbon (C 1s 284.8 eV). P: pellet. SN: supernatant. ND: No detected.

CONCLUSIONS

We were able to demonstrate that thiol-capped AuNPs can experience ligand displacement in the presence of rare earth salts, such as YCl_3, $YbCl_3$ or $TmCl_3$. To the best of our knowledge, this is the first attempt using lanthanide or Yttrium salts to displace thiols from gold surfaces. Although the detailed nature of this phenomenon still remains unclear, we believe these findings create many opportunities in the field of bioimaging and bioanalytical applications in which RE complexes are very well known. Further, the optical changes resulting from the ligand displacement show a notable spectral threshold that may also find applications in the analytical detection of lanthanides. The length of the ligand as well as its nature affect the efficiency of the displacement, a more detailed analysis and quantification are under study now in our lab.

ASSOCIATED CONTENT

Supporting Information. Thiol-capped gold nanoparticle characterization by TEM, UV-Vis and XPS spectroscopy, thiol and citrate displacement by $TmCl_3$ and $YbCl_3$ followed by UV-Vis and XPS spectroscopy are available free of charge.

AUTHOR INFORMATION

Corresponding Authors

*A.E.L.: anabel.lanterna@icloud.com

*J.C.S.: titoscaiano@mac.com

Funding Sources

This work has been supported by the Canada Research Chair Program (Tier I), the Natural Sciences and Engineering Research Council of Canada (Discovery program), and the Canada Foundation for Innovation.

Notes

ORCID Information:

Lanterna, A.E. - 0000-0002-6743-0940

Scaiano, J.C. - 0000-0002-4838-7123

Vanegas, J. P. - 0000-0003-5811-1382

ACKNOWLEDGMENT

J.P.V. is grateful to the ELAP scholarship that supported her research activities in Canada.

REFERENCES

1. Pensa, E.; Cortes, E.; Corthey, G.; Carro, P.; Vericat, C.; Fonticelli, M. H.; Benitez, G.; Rubert, A. A.; Salvarezza, R. C. The Chemistry of the Sulfur-Gold Interface: In Search of a Unified Model. *Acc. Chem. Res.* **2012,** *45* (8), 1183-1192.
2. Zhao, P. X.; Li, N.; Astruc, D. State of the art in gold nanoparticle synthesis. *Coord. Chem. Rev.* **2013,** *257* (3-4), 638-665.
3. Base, T.; Bastl, Z.; Plzak, Z.; Grygar, T.; Plesek, J.; Carr, M. J.; Malina, V.; Subrt, J.; Bohacek, J.; Vecernikova, E.; Kriz, O. Carboranethiol-modified gold surfaces. A study and comparison of modified cluster and flat surfaces. *Langmuir* **2005,** *21* (17), 7776-7785.
4. Sardar, R.; Funston, A. M.; Mulvaney, P.; Murray, R. W. Gold Nanoparticles: Past, Present, and Future. *Langmuir* **2009,** *25* (24), 13840-13851.
5. Giersig, M.; Mulvaney, P. Preparation of Ordered Colloid Monolayers by Electrophoretic Deposition. *Langmuir* **1993,** *9* (12), 3408-3413.
6. Brust, M.; Walker, M.; Bethell, D.; Schiffrin, D. J.; Whyman, R. Synthesis of Thiol-Derivatized Gold Nanoparticles in a 2-Phase Liquid-Liquid System. *J. Chem. Soc. D* **1994,** (7), 801-802.
7. Xue, Y. R.; Li, X.; Li, H. B.; Zhang, W. K. Quantifying thiol-gold interactions towards the efficient strength control. *Nat. Commun.* **2014,** *5*.
8. Kudelski, A. Chemisorption of 2-mercaptoethanol on silver, copper, and gold: Direct Raman evidence of acid-induced changes in adsorption/desorption equilibria. *Langmuir* **2003,** *19* (9), 3805-3813.
9. Hakkinen, H. The gold-sulfur interface at the nanoscale. *Nat. Chem.* **2012,** *4* (6), 443-455.
10. Marin, M. L.; McGilvray, K. L.; Scaiano, J. C. Photochemical Strategies for the Synthesis of Gold Nanoparticles from Au(III) and Au(I) Using Photoinduced Free Radical Generation. *J. Am. Chem. Soc.* **2008,** *130* (49), 16572-16584.
11. Baldock, B. L.; Hutchison, J. E. UV-Visible Spectroscopy-Based Quantification of Unlabeled DNA Bound to Gold Nanoparticles. *Anal. Chem.* **2016,** *88* (24), 12072-12080.
12. Huschka, R.; Zuloaga, J.; Knight, M. W.; Brown, L. V.; Nordlander, P.; Halas, N. J. Light-Induced Release of DNA from Gold Nanoparticles: Nanoshells and Nanorods. *J. Am. Chem. Soc.* **2011,** *133* (31), 12247-12255.
13. Tsai, D. H.; Shelton, M. P.; DelRio, F. W.; Elzey, S.; Guha, S.; Zachariah, M. R.; Hackley, V. A. Quantifying dithiothreitol displacement of functional ligands from gold nanoparticles. *Anal. Bioanal. Chem.* **2012,** *404* (10), 3015-3023.
14. Vanegas, J. P.; Zaballos-Garcia, E.; Gonzalez-Bejar, M.; Londono-Larrea, P.; Perez-Prieto, J. Adenosine monophosphate-capped gold(I) nanoclusters: synthesis and lanthanide ion-induced enhancement of their luminescence. *RSC Adv.* **2016,** *6* (21), 17678-17682.
15. Sedlmeier, A.; Gorris, H. H. Surface modification and characterization of photon-upconverting nanoparticles for bioanalytical applications. *Chem. Soc. Rev.* **2015,** *44* (6), 1526-1560.
16. Ge, X. Q.; Song, Z. M.; Sun, L. N.; Yang, Y. F.; Shi, L. Y.; Si, R.; Ren, W.; Qiu, X.; Wang, H. F. Lanthanide (Gd^{3+} and Yb^{3+}) functionalized gold nanoparticles for in vivo imaging and therapy. *Biomaterials* **2016,** *108*, 35-43.
17. Bear, J.; Choppin, G.; Quagliano, J. Complexes of lanthanide elements with mercapto acetate ligands. *J. Inorg. Nucl. Chem.* **1962,** *24* (12), 1601-1606.

18. Choppin, G. R.; Martinez-Perez, L. A. Thermodynamics of the mercaptopropionate complexes of the lanthanides. *Inorg. Chem.* **1968,** *7* (12), 2657-2659.
19. Dutt, N.; Nag, K.; Seshadri, T. Chemistry of lanthanons—XX complexes of the rare earths with 3-mercapto-1-phenylbut-2-en-1-one. *J. Inorg. Nucl. Chem.* **1969,** *31* (5), 1435-1438.
20. Choppin, G. R. Structure and thermodynamics of lanthanide and actinide complexes in solution. *Pure Appl. Chem.* **1971,** *27* (1-2), 23-42.
21. Gao, J.; Huang, X.; Liu, H.; Zan, F.; Ren, J. Colloidal Stability of Gold Nanoparticles Modified with Thiol Compounds: Bioconjugation and Application in Cancer Cell Imaging. *Langmuir* **2012,** *28* (9), 4464-4471.
22. Chegel, V.; Rachkov, O.; Lopatynskyi, A.; Ishihara, S.; Yanchuk, I.; Nemoto, Y.; Hill, J. P.; Ariga, K. Gold Nanoparticles Aggregation: Drastic Effect of Cooperative Functionalities in a Single Molecular Conjugate. *J. Phys. Chem. C* **2012,** *116* (4), 2683-2690.
23. Lanterna, A. E.; Coronado, E. A.; Granados, A. M. When Nanoparticle Size and Molecular Geometry Matter: Analyzing the Degree of Surface Functionalization of Gold Nanoparticles with Sulfur Heterocyclic Compounds. *J. Phys. Chem. C* **2012,** *116* (11), 6520-6529.
24. Getsova, M.; Todorovsky, D.; Arnaudov, M. Preparation and characterization of yttrium–titanium citrate complexes. *Z. Anorg. Allg. Chem.* **2000,** *626* (6), 1488-1492.
25. Burns, C.; Spendel, W. U.; Puckett, S.; Pacey, G. E. Solution ionic strength effect on gold nanoparticle solution color transition. *Talanta* **2006,** *69* (4), 873-876.
26. Bourg, M. C.; Badia, A.; Lennox, R. B. Gold-sulfur bonding in 2D and 3D self-assembled monolayers: XPS characterization. *J. Phys. Chem. B* **2000,** *104* (28), 6562-6567.
27. Laibinis, P. E.; Whitesides, G. M.; Allara, D. L.; Tao, Y. T.; Parikh, A. N.; Nuzzo, R. G. Comparison of the Structures and Wetting Properties of Self-Assembled Monolayers of Normal-Alkanethiols on the Coinage Metal-Surfaces, Cu, Ag, Au. *J. Am. Chem. Soc.* **1991,** *113* (19), 7152-7167.
28. Castner, D. G.; Hinds, K.; Grainger, D. W. X-ray photoelectron spectroscopy sulfur 2p study of organic thiol and disulfide binding interactions with gold surfaces. *Langmuir* **1996,** *12* (21), 5083-5086.
29. Heister, K.; Zharnikov, M.; Grunze, M.; Johansson, L. S. O. Adsorption of alkanethiols and biphenylthiols on Au and Ag substrates: A high-resolution X-ray photoelectron spectroscopy study. *J. Phys. Chem. B* **2001,** *105* (19), 4058-4061.
30. Malacrida, P.; Casalongue, H. G. S.; Masini, F.; Kaya, S.; Hernandez-Fernandez, P.; Deiana, D.; Ogasawara, H.; Stephens, I. E. L.; Nilsson, A.; Chorkendorff, I. Direct observation of the dealloying process of a platinum-yttrium nanoparticle fuel cell cathode and its oxygenated species during the oxygen reduction reaction. *PCCP* **2015,** *17* (42), 28121-28128.
31. Pomfret, M. B.; Stoltz, C.; Varughese, B.; Walker, R. A. Structural and compositional characterization of yttria-stabilized zirconia: Evidence of surface-stabilized, low-valence metal species. *Anal. Chem.* **2005,** *77* (6), 1791-1795.

TOC Graphic

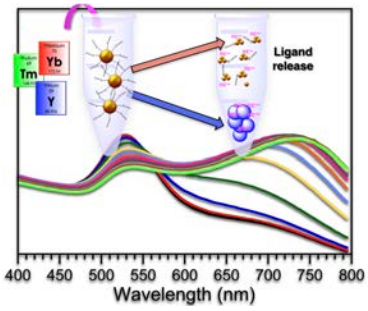
Tm
Yb
Y
Ligand
release
400 450 500 550 600 650 700 750 800
Wavelength (nm)